



NRF2 regulates the sensitivity of human NSCLC cells to cysteine deprivation-induced ferroptosis via FOCAD-FAK signaling pathway

Pengfei Liu^{a,b,*}, Di Wu^c, Jinyue Duan^c, Hexin Xiao^c, Yulai Zhou^c, Lei Zhao^{a,b},
Yetong Feng^{a,b,c,**}

^a Ambulatory Surgical Center, The 2nd Clinical Medical College (Shenzhen People's Hospital) of Jinan University, The 1st Affiliated Hospitals of Southern University of Science and Technology, Shenzhen, 518020, China

^b Integrated Chinese and Western Medicine Postdoctoral Research Station, Jinan University, Guangzhou, 510632, China

^c School of Pharmaceutical Sciences, Jilin University, Changchun, 130012, China

ARTICLE INFO

Keywords:

NRF2
FOCAD
FAK
Ferroptosis
Mitochondria
NSCLC

ABSTRACT

Transcription factor nuclear factor-erythroid 2-like 2 (NRF2) mainly regulates cellular antioxidant response, redox homeostasis and metabolic balance. Our previous study illustrated the translational significance of NRF2-mediated transcriptional repression, and the transcription of *FOCAD* gene might be negatively regulated by NRF2. However, the detailed mechanism and the related significance remain unclear. In this study, we mainly explored the effect of NRF2-FOCAD signaling pathway on ferroptosis regulation in human non-small-cell lung carcinoma (NSCLC) model. Our results confirmed the negative regulation relationship between NRF2 and FOCAD, which was dependent on NRF2-Replication Protein A1 (RPA1)-Antioxidant Response Elements (ARE) complex. In addition, FOCAD promoted the activity of focal adhesion kinase (FAK), which further enhanced the sensitivity of NSCLC cells to cysteine deprivation-induced ferroptosis via promoting the tricarboxylic acid (TCA) cycle and the activity of Complex I in mitochondrial electron transport chain (ETC). However, FOCAD didn't affect GPX4 inhibition-induced ferroptosis. Moreover, the treatment with the combination of NRF2 inhibitor (brusatol) and erastin showed better therapeutic action against NSCLC *in vitro* and *in vivo* than single treatment, and the improved therapeutic function partially depended on the activation of FOCAD-FAK signal. Taken together, our study indicates the close association of NRF2-FOCAD-FAK signaling pathway with cysteine deprivation-induced ferroptosis, and elucidates a novel insight into the ferroptosis-based therapeutic approach for the patients with NSCLC.

1. Introduction

Different from apoptosis, necrosis or autophagic cell death, ferroptosis is a novel programmed cell death pattern, which is mainly results from iron-dependent lipid peroxidation [1,2]. During the process of ferroptosis, glutathione (GSH), the substrate of phospholipid hydroperoxidases, holds an important potential in the regulation of cellular redox contents. Scientists have revealed that the depletion of cellular cysteine or GSH caused by the inhibition of cysteine-glutamate antiporter (system Xc⁻) can disrupt cellular redox homeostasis and lead to ferroptosis finally. Besides, both glutathione peroxidase 4 (GPX4) and

ferroptosis suppressor protein 1 (FSP1) are essential for the clearance of lipid ROS. Therefore, the suppression of GPX4 or FSP1 is also able to induce ferroptosis effectively, without affecting the normal cellular levels of cysteine and GSH [3–5]. In recent years, the position of ferroptosis in different diseases, such as carcinogenesis [6,7], Alzheimer's disease [8], brain injury [9,10], lung injury [11] and ischemia-reperfusion injury [10], has been investigated by different groups. Especially for cancer research and therapy, scientists find that some types of cancer cells are sensitive to ferroptosis inducers, even though they are resistant to the traditional chemotherapy [12]. Therefore, as a novel therapeutic approach, ferroptosis holds promising

* Corresponding author. Ambulatory Surgical Center, The 2nd Clinical medical College (Shenzhen People's Hospital) of Jinan University, The 1st Affiliated Hospitals of Southern University of Science and Technology, Shenzhen, 518020, China.

** Corresponding author. Ambulatory Surgical Center, The 2nd Clinical medical College (Shenzhen People's Hospital) of Jinan University, The 1st Affiliated Hospitals of Southern University of Science and Technology, Shenzhen, 518020, China.

E-mail addresses: pengfeiliu@jnu.edu.cn (P. Liu), fengyt2017@gmail.com (Y. Feng).

<https://doi.org/10.1016/j.redox.2020.101702>

Received 18 April 2020; Received in revised form 19 August 2020; Accepted 23 August 2020

Available online 27 August 2020

2213-2317/© 2020 The Authors.

Published by Elsevier B.V. This is an open access article under the CC BY-NC-ND license

(<http://creativecommons.org/licenses/by-nc-nd/4.0/>).

potential in the treatment of chemotherapy-resistant cancers.

Nuclear factor-erythroid 2-like 2 (NRF2) is one of the most important transcription factors in the regulation of antioxidant response. It binds to the antioxidant response element (ARE) as a heterodimer with small musculoaponeurotic fibrosarcoma proteins (sMAF), and further activates the transcription of ARE-containing genes, such as *NQO1*, *AKR1C1* and *GST* [13,14]. Those NRF2 target genes are essential for eliminating or ameliorating the effects of toxicants/carcinogens and maintaining proper cellular redox homeostasis. Accordingly, activation of the NRF2 pathway by synthetic or naturally-occurring compounds at sub-toxic doses is able to protect against toxic or carcinogenic exposure, thus activation of NRF2 is considered a promising strategy for cancer prevention [13,15,16]. However, many studies have also revealed the “dark” side of NRF2 in cancer therapy. Continuously high level of NRF2 facilitates cancer cell survival and growth, conferring the resistance to current chemotherapy. Therefore, it should be necessary to inhibit NRF2 function during the process of cancer treatment [13,15].

The close connection between NRF2 and ferroptosis have been confirmed by several groups, and lots of genes which inhibits lipid peroxidation, the initiation of ferroptosis, have been identified as NRF2 target genes, such as *HMOX1*, *GPX4* and *SLC7A11* [17–20]. Besides, both glutathione synthesis and iron metabolism can also be regulated by NRF2 signaling pathway effectively [2,20]. Therefore, the inhibition of NRF2 may be also necessary to enhance the sensitivity of cancer cells to ferroptosis.

Over 300 target genes can be upregulated by NRF2 transcriptionally [21]. In contrast, our previous study indicates that the transcription of some genes (such as *MYLK*) also can be directly repressed by NRF2 in an ARE-dependent manner. The transcriptional repression is dependent on the formation of an NRF2-Replication Protein A1 (RPA1)-ARE complex. In this model, RPA1 becomes a novel NRF2-binding partner which competes with sMAF for NRF2 binding. The *in silico* and RNAseq data sets indicates that the NRF2-RPA1-ARE complex may also transcriptionally inhibit other genes, including cancer related gene, *FOCAD* [22].

FOCAD is a kind of focal adhesion proteins that is encoded by *KIAA1797/FOCAD* gene. Some researchers found that the expression level of FOCAD in glioblastoma cell lines and glioblastomas was lower than normal brain tissues, and FOCAD was co-localized with VINCULIN in focal adhesions. In addition, the upregulation of FOCAD expression led to the suppression in colony formation, migration and invasion capacity of cancer cells, indicating the therapeutic potential of FOCAD in cancer treatment [23,24]. However, the detailed function and related mechanism remain unclear for us.

In this study, we mainly explored the significance of NRF2-FOCAD signaling pathway in ferroptosis-based therapy against human non-small-cell lung carcinoma (NSCLC). Our results indicated that FOCAD improved the activity of focal adhesion kinase (FAK), which further promoted the sensitivity of NSCLC cells to cysteine deprivation-induced ferroptosis via enhancing the tricarboxylic acid (TCA) cycle and the activity of Complex I in mitochondrial electron transport chain (ETC). However, FOCAD didn't showed obvious effect on GPX4 inhibition-induced ferroptosis. In addition, we also confirmed the negative regulation relationship between NRF2 and FOCAD, and the treatment with NRF2 inhibitor, brusatol, increased the sensitivity of NSCLC cells to erastin-induced ferroptosis *in vitro* and *in vivo*, which depended on the upregulation of FOCAD partially. Totally, our results elucidate a novel insight into the position of NRF2-FOCAD-FAK signaling pathway in ferroptosis-based treatment for human NSCLC.

2. Materials and methods

All of experiments in this study have been approved by the Committee on the Ethics of Human Subject Research and Animal care of Jinan University. All patients have provided their written informed consent. The ethics committee of Jinan University has approved this consent procedure. In addition, the experiments performed in this study

also conform with The Code of Ethics of the World Medical Association (Declaration of Helsinki).

2.1. Cell culture

Human NSCLC cell lines, A549, NCI-H838 (H838) and NCI-H1703 (H1703), and human bronchial epithelial cell lines, BEAS-2B and NL20, were purchased from the American Type Culture Collection (ATCC, USA). A549 cells were cultured using F-12K medium (Gibco, USA) supplemented with 10% FBS (Gibco, USA), 100 U/mL penicillin and 0.1 g/mL streptomycin (Sigma, USA). H838 and H1703 cell lines were cultured using RPMI-1640 medium (Gibco, USA) supplemented with 10% FBS (Gibco, USA), 100 U/mL penicillin and 0.1 g/mL streptomycin (Sigma, USA). BEAS-2B and NL20 were cultured using Bronchial Epithelial Cell Growth Medium (BEGM, Lonza, USA). All of cells were cultured in a humidified 37 °C incubator with 5% CO₂.

We established *NRF2*^{-/-} and *RPA1*^{-/-} A549 cells using CRISPR/Cas9 method as our previous study [22]. Herein, the same method was applied to established *FOCAD*^{-/-} A549 cell line, and the sgRNA sequences (5'-3') are as follows:

FOCAD-sgRNA-A: 5'-CCAGAGCAGAACGTTTCAGG-3'.

FOCAD-sgRNA-B: 5'-GAGATGTGTTTTATCCACAG-3'.

To establish *FOCAD*-overexpressed cell line, the coding sequence of human *FOCAD* gene was first amplified using PCR (Phusion® High-Fidelity DNA Polymerase, New England BioLabs, USA) and cloned into a pLenti6/V5-D-TOPO® vector (Addgene, USA) subsequently. Meanwhile, the empty pLenti6/V5-D-TOPO® vector was used in the Ctrl group. Then, the lentivirus was prepared using ViraPower™ Lentiviral Expression Systems (K495000, Thermo Fisher, USA). After transduction, the *FOCAD*-overexpressed cells were selected by blasticidin treatment (5 µg/mL, Thermo Fisher, USA).

2.2. Cell viability assay

In our research, the cell viability in each group was detected with Cell Counting Kit-8 (CCK-8, Dojindo, Japan) as the references [25,26]. Briefly, 20 µL of the CCK-8 reagent was added to each well (containing 200 µL of medium) on the 96-well microplate, and the microplate was further incubated at 37 °C for 4 h. Finally, the OD (450 nm) were measured in different groups (n = 3). The cell viability in the control group (without any treatment) was regarded as “100%”, and the relative cell viability of the other groups was calculated respectively.

2.3. Real-time qRT-PCR

Real-time qPCR was performed as our previously described [11,22,27]. In this study, β-actin was used in the qPCR normalization, and all of experiments were measured in triplicate. Primer sequences (5'-3') are as follows:

FOCAD-Forward 5'-CCAGGTGCCAAATCTGATTCC-3'.

FOCAD-Reverse 5'-TGGTGTGGTCCAAGTAGTTGT-3'.

HMOX1-Forward 5'-AACTTTCAGAAGGGCCAGGT-3'.

HMOX1-Reverse 5'-CTGGGCTCTCCTTGTGTC-3'.

GPX4-Forward 5'-GAGGCAAGACCGAAGTAAACTAC-3'.

GPX4-Reverse 5'-CCGAAGCTGTTACAGGGAA-3'.

SLC7A11-Forward 5'-TCTCAAAGGAGGTTACTCTGC-3'.

SLC7A11-Reverse 5'-AGACTCCCCTCAGTAAAGTGAC-3'.

AKR1B1-Forward 5'-TTTTCCCATTTGGATGAGTCCG-3'.

AKR1B1-Reverse 5'-CCTGGAGATGGTTGAAGTTGG-3'.

FTH1-Forward 5'-CCCCATTGTGTGACTTCAT-3'.

FTH1-Reverse 5'-GCCCGAGGCTTAGCTTTTCAAT-3'.

FTL-Forward 5'-CAGCCTGGTCAATTTGTACTC-3'.

FTL-Reverse 5'-GCCAATTCGCGGAAGAAGTG-3'.

PTGS2-Forward 5'-CGGTGAAACTCTGGCTAGACAG-3'.

PTGS2-Reverse 5'-GCAAACCGTAGATGCTCAGGGA-3'.

β-actin-Forward 5'-CCAGAGCAAGAGAGG-3'.

β -actin-Reverse 5'-GTCCAGACGCAGGATG-3'.

2.4. Transfection of small interfering RNA (siRNA)

In our study, Hiperfect (Qiagen, USA) was used for the transfection of siRNA as the manufacturer's instructions. NRF2-siRNA (SI03246950), FOCAD-siRNA 5# (SI04289747), FOCAD-siRNA #6 (SI04309543), and Negative control-siRNA (1022076) were purchased from Qiagen (USA).

2.5. MitoTracker staining and JC-1 staining

Both MitoTracker Green Probe and JC-1 Mitochondrial Potential Sensor were purchased from Invitrogen (USA). 1×10^5 cells were harvested in medium and incubated with MitoTracker Green Probe (0.2 μ M) or JC-1 Mitochondrial Potential Sensor (1 μ g/mL) for 30 min in 37 °C. Then the cells were washed once with fresh medium and analyzed by flow cytometry.

2.6. Western blot and immunohistochemistry (IHC) staining

In the present study, western blot and IHC staining were carried out as our previous description [28,29]. For western blot, 20 μ g of protein sample was added in each lane and separated using 7% or 12% SDS-PAGE gel. Then, the sample in gel was transferred to nitrocellulose membranes, which was further blocked using 5% bovine serum albumin. The membrane was incubated with primary antibodies overnight at 4 °C. In the present study, the primary antibodies used were: anti-FOCAD (1:1000; Biorbyt, orb450232, UK), anti-NRF2 (1:1000; Proteintech, 16396-1-AP, USA), anti-NQO1 (1:1000; Santa Cruz, sc-376023, USA), anti-RPA1 (1:1000; Santa Cruz, sc-48425, USA), anti-sMAF (1:3000; Santa Cruz, sc-166548, USA), anti-FAK (1:2000; Abcam, ab40794, USA), anti-pFAK (phospho Y397) (1:2000; Abcam, ab81298, USA), anti-TIM23 (1:2000; Abcam, ab230253, USA), and anti-GAPDH (1:3000; Santa Cruz, sc-47724, USA). Then, the membrane was incubated with HRP labeled secondary antibodies, and the protein bands were visualized using an enhanced chemiluminescence kit (SuperSignal West Femto Maximum Sensitivity Substrate, Thermo Fisher Scientific, USA) and ChemiDoc Imagers (Bio-Rad Laboratories, USA). For IHC, the paraffin embedded tissues were sectioned at a 5 μ m thickness and then baked and deparaffinized. After blocked with 5% BSA, the slice was incubated with primary antibodies overnight at 4 °C, and non-specific IgG was used in the negative control group. Then, the staining was performed using the EnVision + System-HRP kit (Dako) according to the manufacturer's instructions. Primary antibodies used were: anti-NRF2 (1:100; Proteintech, 16396-1-AP, USA) and anti-FOCAD (1:300, Thermo Fisher, PA5-63051, USA).

2.7. Detection of malondialdehyde (MDA) and 4-hydroxynonenal (4-HNE)

In our study, the MDA and 4-HNE were measured to evaluate ferroptosis level in each group. The concentration of MDA and 4-HNE in cell lysates were measured using the Lipid Peroxidation (MDA) Assay Kit (MAK085, Sigma-Aldrich, USA), and Lipid Peroxidation (4-HNE) Assay Kit (ab238538, Abcam, USA) according to the manufacturer's instructions. First, the cells or tissues were lysed using the lysis buffer, and the insoluble material was removed via centrifuge. For MDA detection, the samples were mixed with thiobarbituric acid and incubated at 95 °C for 1 h. The absorbance at 532 nm were measured to determine the MDA concentration. For 4-HNE detection, the samples were added into the 4-HNE Conjugate coated plate and incubate for 10 min. Then, the conjugated 4-HNE was incubated with Anti-4-HNE antibody and Secondary Antibody-HRP. Finally, Substrate Solution was added and the absorbance at 450 nm were measured. Herein, the amount of MDA or 4-HNE was calculated in 1×10^6 cells or 1 mg tissues after treatment.

2.8. BODIPY staining

To further evaluate lipid peroxidation in each group, BODIPY staining was used in our research. The cells were washed with PBS, and incubated with 1 μ M BODIPY 493/503 (Thermo Fisher, USA) for 0.5 h at 37 °C. Then the cells were washed with PBS and analyzed by Flow cytometry (BD Biosciences, USA).

2.9. TCA cycle assay

In this research, the key metabolites in TCA cycle, α -Ketoglutarate (α -KG) and succinate (Suc), were measured respectively to evaluate the TCA cycle in different groups. Herein, α -KG was detected using α -Ketoglutarate Assay Kit (MAK054, Sigma, USA), and Suc was measured with Succinate Colorimetric Assay Kit (MAK184, Sigma, USA) according to the manufacturer's instructions.

2.10. Evaluation of mitochondrial ETC activity

In our study, mitochondria was isolated from cell samples with Mitochondria Isolation Kit for Cultured Cells (ab110170, Abcam, USA). Then, the activity of Complex I to IV in mitochondrial ETC was measured using Complex I Enzyme Activity Assay Kit (ab109721, Abcam, USA), Complex II Enzyme Activity Assay Kit (ab109908, Abcam, USA), Mitochondrial Complex III Activity Assay Kit (K520-100, Biovision, USA), and Complex IV Enzyme Activity Assay Kit (ab109909, Abcam, USA) according to the manufacturer's instructions respectively.

2.11. Luciferase activity assay

Luciferase activity was detected using the Dual-luciferase Reporter Assay System (Promega, USA). For relative luciferase activity assay, the value of Firefly-luciferase was normalized to the value of Renilla-luciferase. Briefly, 1×10^5 A549 cells/well were seeded into a 24-well plate and cultured overnight. Then 0.45 μ g of pGL3-FOCAD-ARE plasmid and 0.05 μ g of hRluc/TK plasmid were cotransfected into the cell using Lipofectamine 3000. 24 h later, the cells were treated with different compounds for another 16 h. Finally the cells were lysed using Passive lysis buffer (Promega, USA), and both Firefly-luciferase and Renilla-luciferase values were measured using Dual luciferase assay kit (Promega, E1910, USA) and luminometer (Model TD-20/20, Turner BioSystems, CA).

2.12. Biotin-DNA pull-down

Biotin-DNA pull-down was carried out as reported previously [22,30]. Briefly, the cell samples were lysed using RIPA buffer containing 1 mM DTT (Sigma, USA), 1 mM phenylmethylsulfonyl fluoride (PMSF, Sigma, USA) and 1% protease inhibitor cocktail (Sigma, USA), and the total cell lysates were pre-cleared using streptavidin beads (Invitrogen, USA) and further incubated with 2 μ g biotinylated DNA probes which spanned the ARE containing sequences in the promoter regions of human FOCAD gene (41 bp). The DNA-protein complexes were pulled down using streptavidin beads. After washed for 3 times, the complexes were resolved on an SDS-PAGE gel, and subjected to western blot assay.

2.13. Xenograft mouse model

In our study, NOG mouse (Charles River Laboratories, China) were used to establish xenograft mouse model. The 6 week-old male mice were injected with A549 cells (100 μ L containing 5×10^6 cells/mouse, i. h.). After the volume of tumor reached about 100–120 mm³, the mice were divided into 4 different groups (n = 5) for both FOCAD-wild type (FOCAD-WT) and FOCAD-knockout (FOCAD-KO) cells respectively. Brusatol (0.5 mg/kg), erastin (15 mg/kg) and RSL3 (100 mg/kg) were dissolved in 5% DMSO/corn oil. Brusatol and Erastin injected into the

mice intraperitoneally, and RSL3 was administrated intratumorally (twice in one week) for 4 weeks. Then, the mice were sacrificed and tumor weight in different groups was measured respectively. Besides, the survival rate within 120 days was also evaluated in each group (n = 10).

2.14. Statistical analysis

In our study, all of results were presented as mean ± SD (n = 3), and the statistical analysis was performed using SPSS 17.0. Herein, the unpaired Student's t-tests were applied to compare the means between two different groups, and one-way ANOVA with Bonferroni's correction was used to compare the means among three or more groups. Besides, the one-tailed test was applied in the Student's t-test, and p value lower than 0.05 was considered significant statistically.

3. Results

3.1. NRF2 negatively regulates FOCAD expression

To explore the cross-talk between FOCAD and NRF2 in NSCLC cells,

the cancer tissues and paracancer tissues from 6 different NSCLC patients were harvested for IHC staining first. The results from most patients (Patient-001 to Patient-005) except Patient-006, indicated the high expression of NRF2 and low expression of FOCAD in cancer tissues, while the opposite results existed in paracancer tissues (Fig. 1A–C). Therefore, there could be a negative regulation relationship between NRF2 and FOCAD. To further confirm the hypothesis, two bronchial epithelial cell lines (BEAS-2B and NL20) were treated with sulforaphane (NRF2 activator), and three NSCLC cell lines (H838, H1703 and A549) were treated with brusatol (NRF2 inhibitor). The immunoblot results indicated that the treatment with sulforaphane increased the expression of NRF2 and NQO1 (NRF2 target gene), which were downregulated by brusatol treatment. However, the protein level of FOCAD showed an opposite response to the compounds treatment (Figs. S1A–S1D). The effect of brusatol in different concentrations on FOCAD were analyzed in A549 cells, and a concentration-dependent response was showed on the effect of brusatol on FOCAD expression in A549 cells (Fig. 2A–B). In addition, we established NRF2-knockdown and NRF2-knockout cells using NRF2 specific siRNA and CRISPR/Cas9, and the immunoblot and qPCR results also indicated that FOCAD could be a negatively regulated NRF2 target gene (Fig. 2C–D).

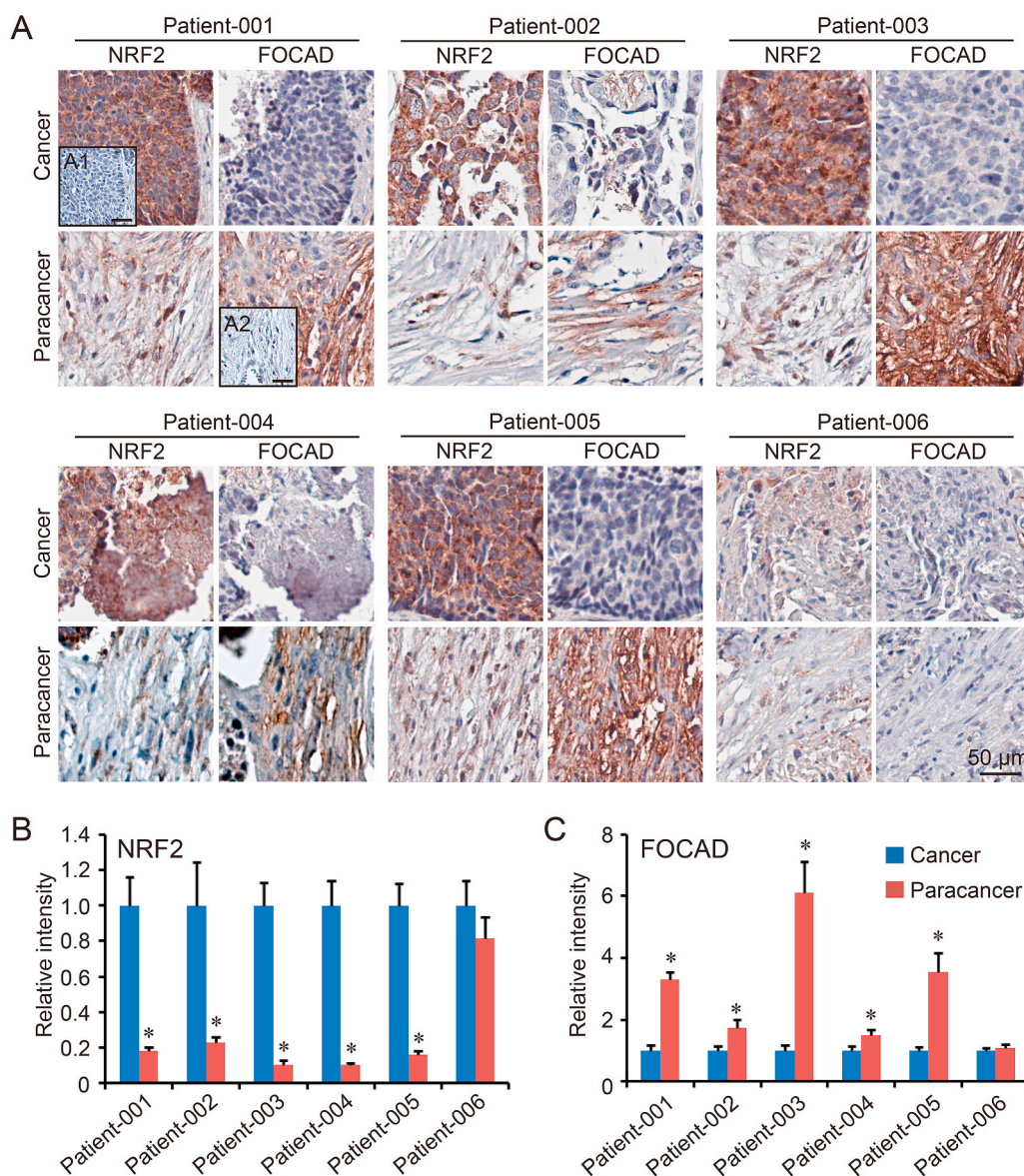


Fig. 1. The expression of NRF2 and FOCAD in human NSCLC tissues. The cancer tissues and paracancer tissues from 6 NSCLC patients (Patient-001 to Patient-006) were harvested for NRF2 and FOCAD via IHC staining (A). In the negative control, non-specific IgG was used to replace the first antibody. The cancer slice from patient-001 was used in the negative control of NRF2 staining (A1), and the paracancer slice from patient-001 was used in the negative control of FOCAD staining (A2). The relative intensity of NRF2 (B) and FOCAD (C) were calculated respectively, and the level in Cancer group was considered as “1”. Results were expressed as mean ± SD, and the P value less than 0.05 was considered statistically significant. *: P < 0.05 compared between cancer tissue and paracancer.

To analyze the potential involvement of the ARE in this repressive mechanism, an ARE-like sequence, TTGATGCAGCA (-4705~-4695), was identified in the promoter region of *FOCAD* gene. Because the core sequence of ARE was regarded as 5'-TGA(C/T)nnnGC(A/G)-3' [31], the mutation of "TGA" and "GC" was performed to abolish the function of ARE. Using biotinylated DNA probes (41 bp) of either wild type ARE (Biotin-*FOCAD*-ARE-WT) or mutated ARE (Biotin-*FOCAD*-ARE-MU), we found that NRF2 and sMAF specifically bound to wild type ARE, but not to mutated ARE. Either mutation or NRF2 knockout decreased the binding ability of RPA1 (Fig. 2E). Luciferase activity was measured in A549-WT, A549-NRF2^{-/-} and A549-RPA1^{-/-} cells transfected with luciferase reporters containing 41 bp-ARE in *FOCAD* gene promoter region. NRF2 inhibitors (brusatol and ML385) treatment increased the relative luciferase activity in A549-WT cells, which could be abolished by NRF2 knockout. Moreover, RPA1 knockout switched the negative regulation to positive regulation, indicating the function of

NRF2-RPA1-ARE complex in the transcription of *FOCAD* gene (Fig. 2F).

3.2. *FOCAD* enhances the sensitivity of NSCLC cells to the ferroptosis induced by cysteine deprivation, but not GPX4 inhibition

The function of NRF2 on ferroptosis has been confirmed by several groups. However, the role of *FOCAD* in ferroptosis regulation is still unclear. Therefore, to explore the position of *FOCAD* gene in ferroptosis, *FOCAD* knockout model was established in A549 cell line. Meanwhile, ferroptosis model was induced by system Xc⁻ inhibitor, erastin, and GPX4 inhibitor, RSL3, in *FOCAD*-Wild type (*FOCAD*-WT) and *FOCAD*-knockout (*FOCAD*-KO) A549 cells respectively. Our results indicated that the cell viability was suppressed by both erastin and RSL3. *FOCAD* knockout rescued the inhibition caused by erastin-induced ferroptosis, but not RSL3-induced ferroptosis (Fig. 3A). In addition, the basal levels of MDA and 4-HNE, two ferroptosis makers, didn't show obvious

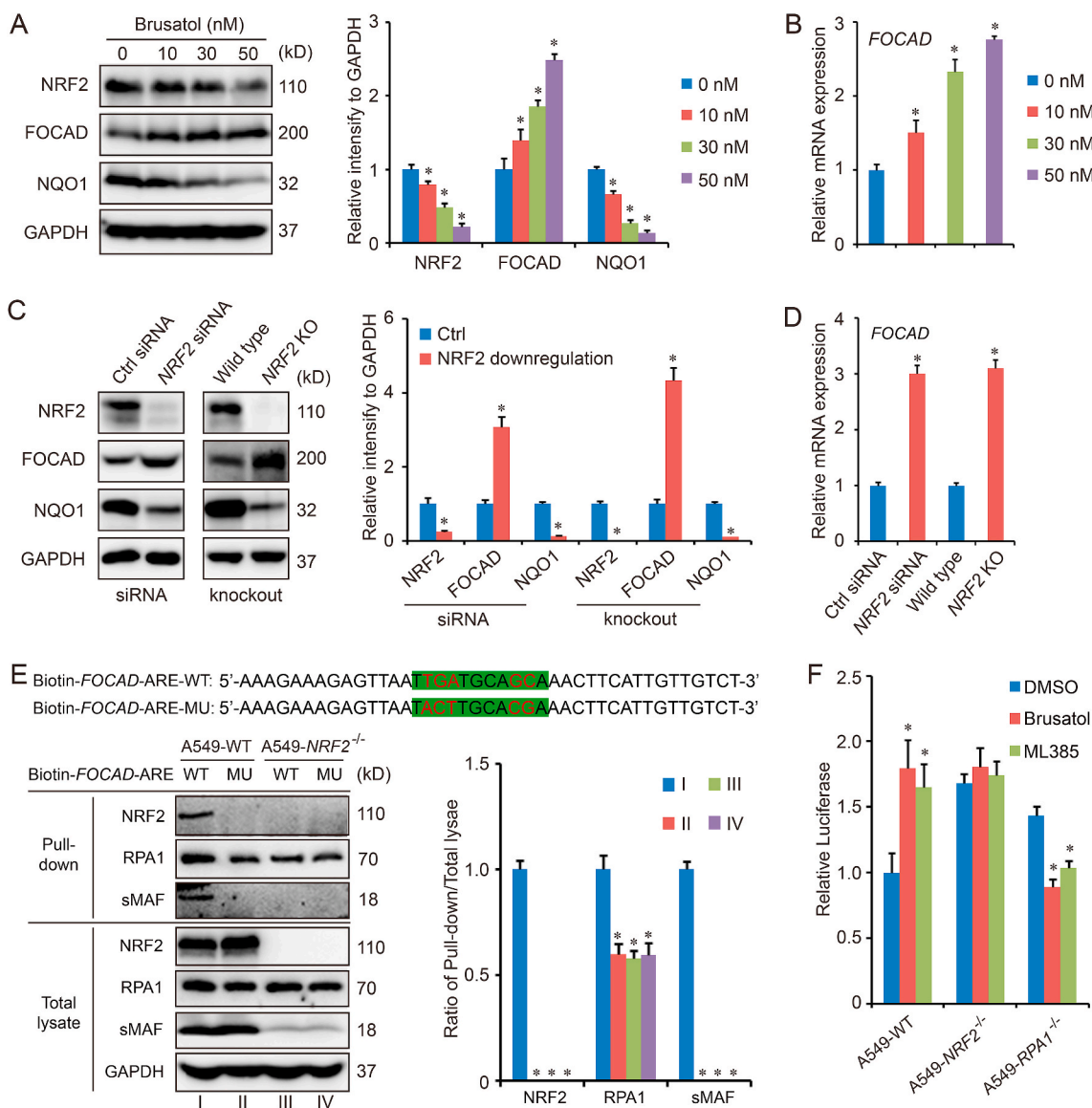


Fig. 2. NRF2 negatively regulates the expression of *FOCAD*. To downregulate the expression of NRF2, A549 cells were treated with brusatol (10 nM, 30 nM, 50 nM for 16 h) (A–B) or siRNA (10 nM for 48 h) (C–D). NRF2 knockout (KO) cell line was also established using CRISPR/Cas9 (C–D). Then, the cell samples were harvested for western blot (A and C) and qPCR detection (B and D). In addition, biotinylated DNA probes (41 bp) spanned the ARE containing sequences in the promoter regions of human *FOCAD* gene, and the DNA-protein complexes were pulled down using streptavidin beads for immunoblot detection (E). To confirm the model, RPA1 knockout cell line (A549-RPA1^{-/-}) was also established and pGL3-*FOCAD*-ARE plasmid and hRluc/TK plasmid were cotransfected into the cell using Lipofectamine 3000. 24 h later, the cells were treated with brusatol (50 nM for 16 h) or ML385 (5 μM for 16 h) for luciferase activity assay (F). Results were expressed as mean ± SD (n = 3), and the P value less than 0.05 was considered statistically significant. *: P < 0.05 compared with the control (without any treatment) group.

difference between *FOCAD*-WT group and *FOCAD*-KO group, but *FOCAD* knockout reduced the sensitivity of A549 cells to the ferroptosis induced by erastin (Fig. 3B–C). Besides, the expression of *PTGS2* (a marker gene of ferroptosis) and lipid peroxidation, were measured using qPCR and flow cytometry respectively. The results were similar to MDA and 4-HNE detection (Fig. 3D–F), indicating that *FOCAD* could strengthen the sensitivity of A549 cells to ferroptosis induced by cysteine deprivation.

Because the metabolic phenotype in cancer cells is different from that of primary cells, the position of *FOCAD* in ferroptosis was further evaluated in BEAS-2B cells. *FOCAD*-knockdown was induced by *FOCAD* specific siRNA transfection (Figs. S2A–S2B). Our results showed that *FOCAD* knockdown relieved the inhibition caused by erastin-induced ferroptosis, but not RSL3-induced ferroptosis in BEAS-2B cells (Figs. S2C–S2F), which was similar to the results in A549 cells.

3.3. *FOCAD* promotes mitochondrial TCA cycle and improves the activity of complex I in mitochondrial ETC

The essential position of TCA cycle and glutaminolysis have been identified in cysteine deprivation-induced ferroptosis, and both the absence of glutamine and the block of TCA cycle can relieve the cysteine deprivation-induced ferroptosis [32]. Therefore, the effect of *FOCAD* on

TCA cycle was evaluated in our study. Our results showed that the basal levels of α -Ketoglutarate (α -KG) and succinate (Suc), downstream metabolites of glutaminolysis, were lower in *FOCAD*-KO group than *FOCAD*-WT group. The absence of glutamine effectively decreased the levels of α -KG and Suc, and the cellular Suc level could be increased by α -KG treatment in both *FOCAD*-WT and *FOCAD*-KO group, while *FOCAD*-KO group showed weaker response to the glutamine or α -KG regulation than *FOCAD*-WT group, suggesting the importance of *FOCAD* in the maintenance of mitochondrial TCA cycle (Fig. 4A–C). Besides, the effect of glutamine starvation and α -KG treatment on erastin-induced ferroptosis was analyzed in *FOCAD*-WT and *FOCAD*-KO cells. We found that the ferroptosis was aggravated by α -KG treatment, but was rescued by glutamine starvation significantly, and the difference between *FOCAD*-WT group and *FOCAD*-KO group was also reduced by the starvation of glutamine (Fig. 4D–G). Totally, those results indicated that the effect of *FOCAD* on the sensitivity of NSCLC cells to cysteine deprivation-induced ferroptosis, partially depended on the regulation of mitochondrial TCA cycle.

Besides mitochondrial TCA cycle, the different components (Complex I to IV) in mitochondrial ETC are also essential for cysteine deprivation-induced ferroptosis. Mitochondrial ETC is formed by a series of electron transporters, and it's necessary for ATP production and

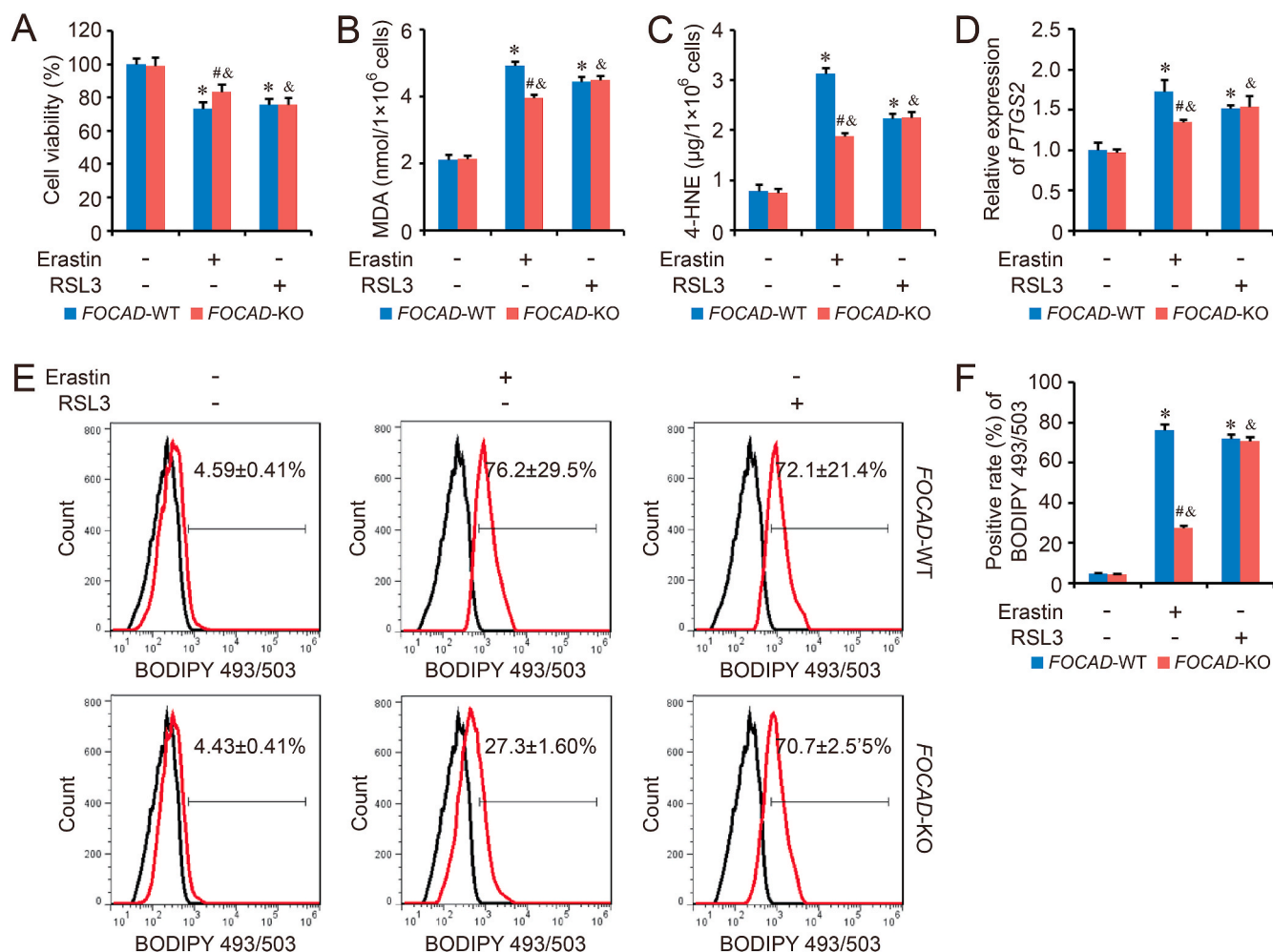


Fig. 3. *FOCAD* knockout relieves the cysteine deprivation-induced ferroptosis. The cysteine deprivation-induced ferroptosis model and GPX4 inhibition-induced ferroptosis model was established by erastin (5 μM for 24 h) and RSL3 (1 μM for 24 h) in *FOCAD*-wild type (*FOCAD*-WT) and *FOCAD*-knockout (*FOCAD*-KO) NSCLC cells respectively. Then, cell viability was evaluated using CCK-8 method (A). To analyze the ferroptosis level, MDA (B) and 4-HNE (C) levels were measured in different groups. The expression of *PTGS2* (D) and lipid peroxidation (E–F) were detected using qPCR and BODIPY staining respectively. Results were expressed as mean ± SD (n = 3), and the P value less than 0.05 was considered statistically significant. *: P < 0.05 compared with the *FOCAD*-WT group in Erastin(–)RSL3(–) condition. #: P < 0.05 compared between *FOCAD*-WT group and *FOCAD*-KO group in same condition. &: P < 0.05 compared with the *FOCAD*-KO group in Erastin(–)RSL3(–) condition.

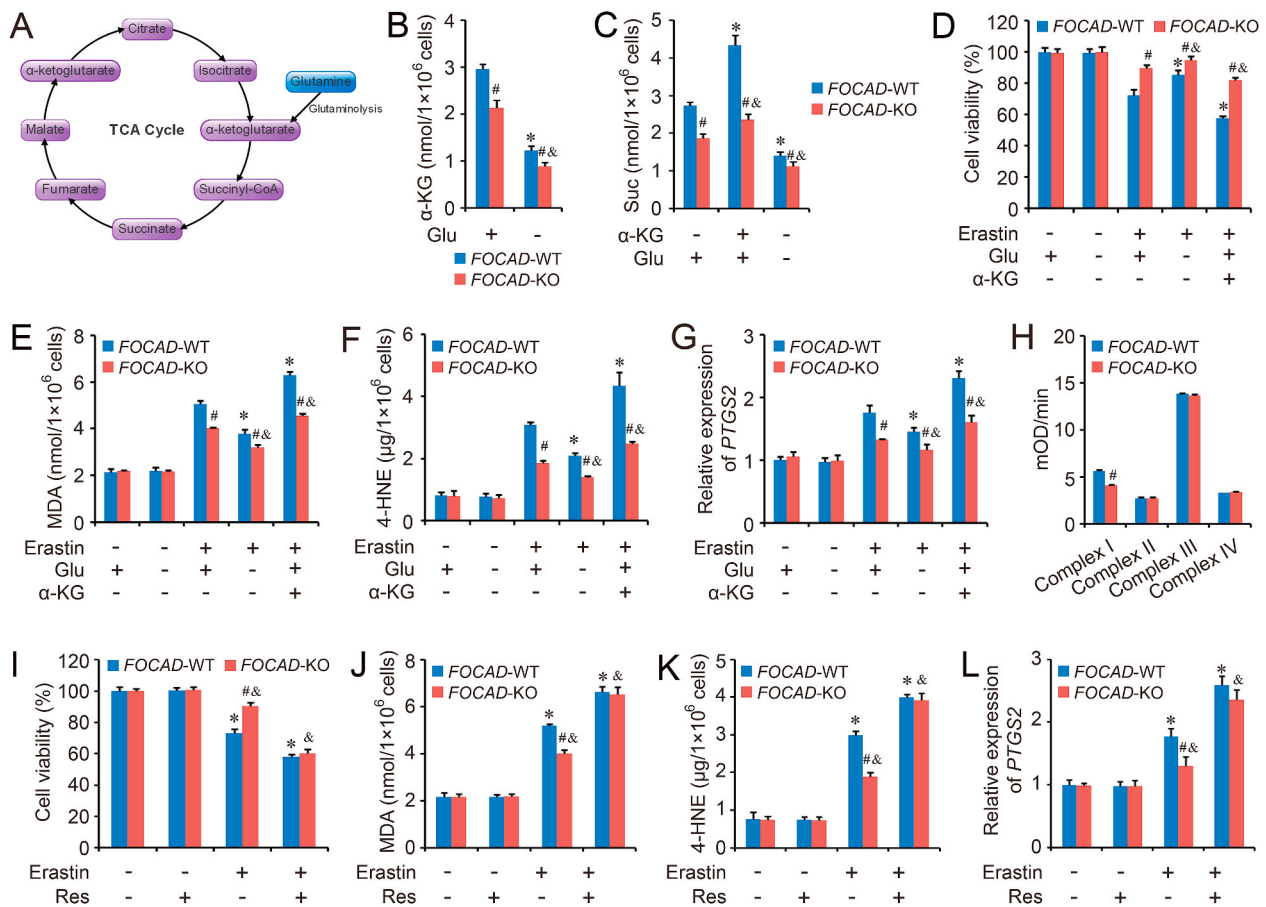


Fig. 4. FOCAD is essential for mitochondrial TCA cycle and Complex I activity in mitochondrial ETC. An overview of TCA cycle was showed in Fig. 4A. Herein, the ferroptosis model was induced by erastin (5 μ M for 24 h) treatment. Meanwhile, the cells were treated with glutamine (Glu) starvation or α -Ketoglutarate (α -KG, 5 mM). The levels of α -KG (B) and succinate (Suc) (C) were measured in each group. In addition, cell viability (D), MDA (E), 4-HNE (F) as well as the expression of *PTGS2* (G) were also measured respectively to evaluate ferroptosis in different groups. In addition, the activity of different complexes (Complex I to IV) in mitochondrial ETC were analyzed respectively (H), and the raw curve figures were showed in Fig. S4. Meanwhile, the cells were treated with Complex I activator, Resveratrol (Res, 5 μ M for 24 h), then cell viability (I), MDA (J) and 4-HNE (K), as well as the expression of *PTGS2* (L) were also evaluated respectively. Results were expressed as mean \pm SD (n = 3), and the P value less than 0.05 was considered statistically significant. *: P < 0.05 compared with the *FOCAD*-WT group in the first condition. #: P < 0.05 compared between *FOCAD*-WT and *FOCAD*-KO group in same condition. &: P < 0.05 compared with the *FOCAD*-KO group in the first condition.

energy generation. Herein, the influence of FOCAD on different ETC components was detected in *FOCAD*-WT and *FOCAD*-KO cells. Our results indicated that FOCAD knockout didn't affect the intactness of mitochondria (Figs. S3A–S3B) or the total amount of mitochondria (Figs. S3C–S3D). However, the activity of Complex I in mitochondrial ETC was inhibited by *FOCAD* knockout, and no obvious difference could be found about the activity of Complex II, Complex III or Complex IV between *FOCAD*-WT group and *FOCAD*-KO group (Fig. 4H and Fig. S4). Therefore, FOCAD might regulate ferroptosis via affecting the activity of Complex I in mitochondrial ETC. To confirm the hypothesis, the activator of Complex I in mitochondrial ETC, resveratrol (Res) [33], was applied herein. After Res treatment, the activity of Complex I was improved significantly, and no obvious difference existed between *FOCAD*-WT group and *FOCAD*-KO group (Fig. S5A). In addition, the level of α -KG and Suc also reached to similar level in *FOCAD*-WT and *FOCAD*-KO cells after Res treatment, indicating that the effect of FOCAD on mitochondrial TCA cycle mainly depended on the regulation of Complex I activity in mitochondrial ETC (Fig. S5B). More importantly, Res promoted the erastin-induced ferroptosis in both *FOCAD*-WT group and *FOCAD*-KO group, and there were no obvious difference between *FOCAD*-WT group and *FOCAD*-KO group after the Res treatment (Fig. 4I–L).

3.4. FOCAD regulates mitochondrial TCA cycle and ETC via FAK signaling

Even though our results indicates the function of FOCAD in the regulation of mitochondrial TCA cycle and ETC, the detailed mechanism is still unclear, and no evidences reveal the direct link between FOCAD and mitochondria. However, the position of focal adhesion kinase (FAK) in mitochondrial regulation has been demonstrated by several groups [34–37]. Therefore, the relationship between FOCAD and FAK was further investigated in our study because of the role of FOCAD in focal adhesion. We found that *FOCAD* knockout indeed decreased the level of phospho-FAK (pFAK), but not total FAK (Fig. 5A–B). To confirm this results, *FOCAD* overexpressed A549 cell line was established, and the detection indicated FOCAD overexpression increased the amount of pFAK as well as the ratio of pFAK/FAK, which could be abolished totally by the treatment of PF-573228 (PF), a FAK signaling inhibitor (Fig. 5C–D). Besides, FOCAD overexpression (*FOCAD*-OE) also enhanced the mitochondrial TCA cycle (Fig. 5E–F) and the Complex I activity in mitochondrial ETC (Fig. 5G and Fig. S6), and PF treatment reduced the basal level of α -KG and Suc (Fig. 5E–F). No obvious difference in TCA cycle or Complex I activity existed between *FOCAD*-WT group and *FOCAD*-OE group after PF treatment (Fig. 5E–G and Fig. S6). In addition, we also found the overexpression of FOCAD increased the sensitivity of

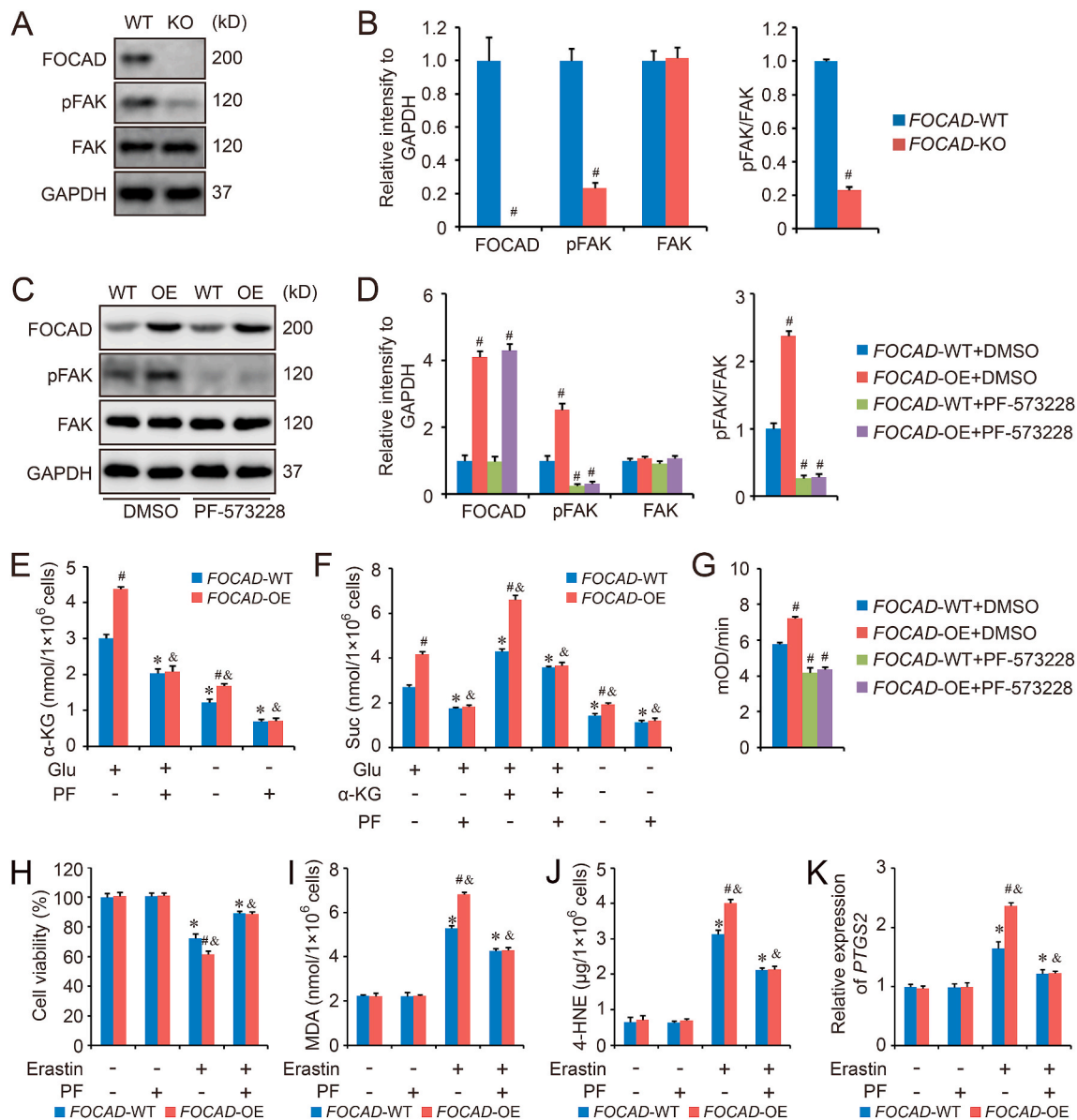


Fig. 5. FOCAD promotes mitochondrial function via enhancing the activity of FAK. FOCAD-knockout (FOCAD-KO) cell line was established by CRISPR/CAS9 in A549 cells, and the effect of FOCAD on FAK activity was evaluated by western blot (A). The relative quantification of immunoblot results was showed in 5B. FOCAD overexpression was induced by lentivirus transduction in A549 cells, and both FOCAD-wild type (FOCAD-WT) and FOCAD-overexpressed (FOCAD-OE) cells were treated with FAK inhibitor, PF-573228 (3 μM for 24 h). Then the cells were harvested for western blot detection (C–D). Besides, the function of PF-573228 on mitochondrial TCA cycle (E–F) and Complex I activity in mitochondrial ETC (G and Fig. S6) were also evaluated respectively. The ferroptosis model was induced by erastin (5 μM for 24 h) treatment, and the cell viability (H), MDA (I) and 4-HNE (J), as well as the expression of PTGS2 (K) were measured respectively to evaluate ferroptosis in different groups. Results were expressed as mean ± SD (n = 3), and the P value less than 0.05 was considered statistically significant. In Fig. 5A–D and 5G, #: P < 0.05 compared with FOCAD-WT/FOCAD-WT + DMSO group. In Fig. 5E–F and 5H–5K, *: P < 0.05 compared with the FOCAD-WT group in the first condition. #: P < 0.05 compared between FOCAD-WT group and FOCAD-OE group in same condition. &: P < 0.05 compared with the FOCAD-OE group in the first condition.

A549 cells to cysteine deprivation-induced ferroptosis, and the co-treatment with PF could rescue the cell death induced by erastin effectively, which was consistent with the results about mitochondrial TCA cycle or Complex I activity (Fig. 5H–K).

3.5. Brusatol enhances the anti-cancer effect of erastin and RSL3 in vitro and in vivo

Brusatol, the first NRF2 inhibitor, can enhance the efficacy of chemotherapy via inhibiting NRF2 signaling pathway [38]. As lots of anti-ferroptosis genes are considered as NRF2 target genes, brusatol may also be available to promote the anti-cancer ability of ferroptosis

inducers. We detect the effect of brusatol on the transcription of several anti-ferroptosis genes (HMOX, GPX4, SLC7A11, AKR1B1, FTH1 and FTL), and the results indicated that the mRNA level of those genes were downregulated by brusatol treatment significantly, although no difference could be found between FOCAD-WT group and FOCAD-KO group (Fig. 6A). In addition, as our previous results, brusatol treatment improved the level of FOCAD and pFAK. FOCAD knockout inhibited the ratio of pFAK/FAK, and also abolished the effect of brusatol treatment (Fig. 6B–C). Moreover, brusatol increased the level of α-KG and Suc (Fig. 6D–E), and enhanced the activity of Complex I in FOCAD-WT cells (Fig. 6F and Fig. S7), but not in FOCAD-KO cells, indicating that the effect of brusatol on mitochondrial TCA cycle and ETC depended on the

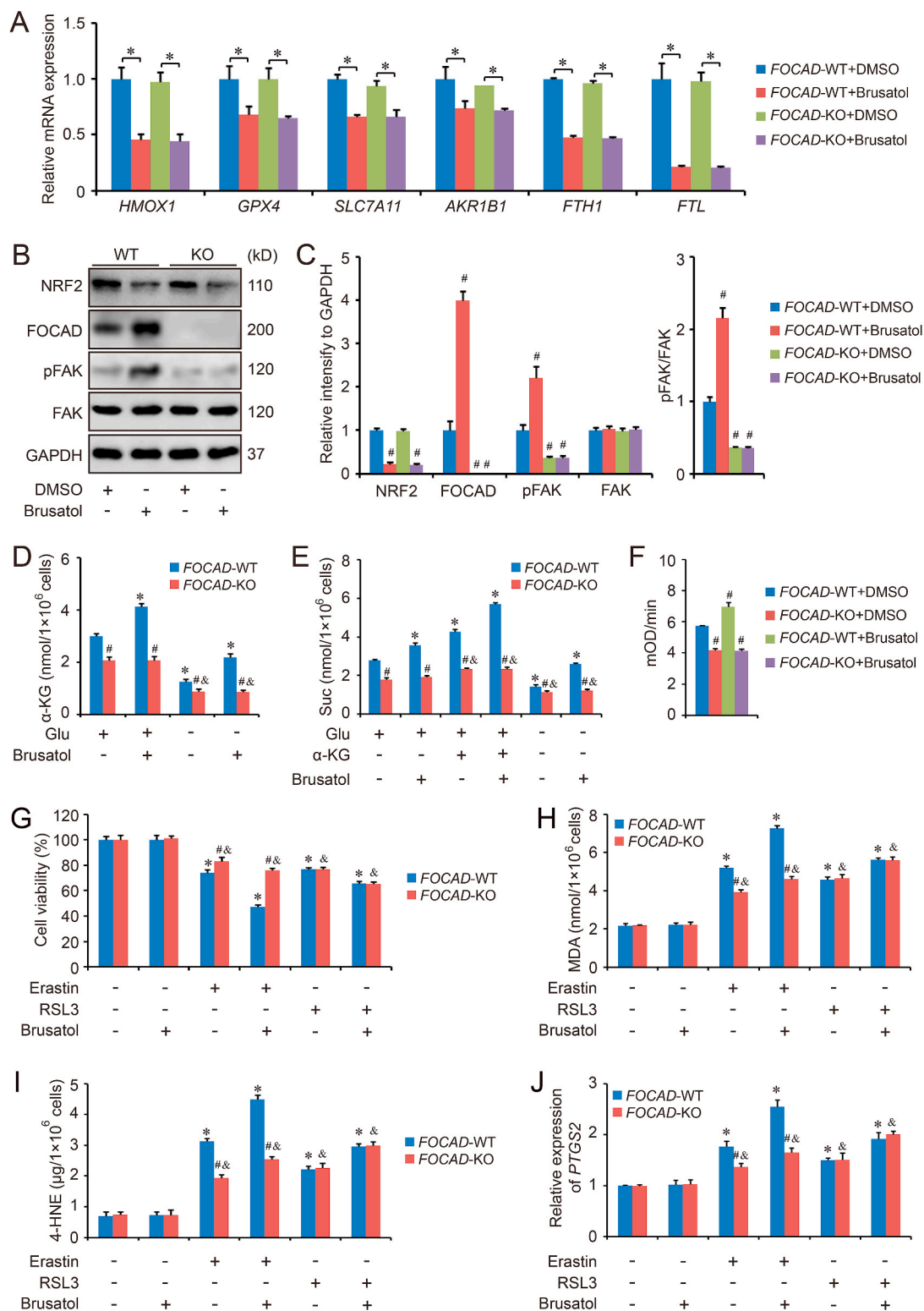


Fig. 6. Brusatol promotes erastin-induced ferroptosis via FOCAD-FAK signaling partially. Both *FOCAD*-wild type (*FOCAD*-WT) and *FOCAD*-knockout (*FOCAD*-KO) cells were treated with brusatol (50 nM for 16 h in qPCR detection and 50 nM for 24 h in western blot detection). Then the cells were harvested for qPCR (A) and western blot detection (B–C). Besides, the function of brusatol on mitochondrial TCA cycle (D–E) and Complex I activity in mitochondrial ETC (F and Fig. S7) were also evaluated respectively. The ferroptosis model was induced by erastin (5 μ M for 24 h) or RSL3 (5 μ M for 24 h) treatment, and the cell viability (G), MDA (H), 4-HNE (I), as well as the expression of *PTGS2* (J) were measured respectively to evaluate ferroptosis in different groups. Results were expressed as mean \pm SD (n = 4), and the P value less than 0.05 was considered statistically significant. In Fig. 6A, *: P < 0.05 compared between two different groups. In Fig. 6C and F, #: P < 0.05 compared with *FOCAD*-WT + DMSO group. In Fig. 6D–E and 6G–6J, *: P < 0.05 compared with the *FOCAD*-WT group in the first condition. #: P < 0.05 compared between *FOCAD*-WT group and *FOCAD*-KO group in same condition. &: P < 0.05 compared with the *FOCAD*-KO group in the first condition.

regulation of FOCAD.

Meanwhile, we also evaluated the response to erastin/RSL3-induced ferroptosis in *FOCAD*-WT and *FOCAD*-KO cells treated with brusatol. The results showed that brusatol treatment increased the sensitivity of both *FOCAD*-WT and *FOCAD*-KO cells to erastin/RSL3-induced ferroptosis. Differently, *FOCAD* knockout blocked the effect of brusatol in erastin-induced ferroptosis in some degree, but not in RSL3-induced

ferroptosis (Fig. 6G–J). In addition, the therapeutic action of erastin/RSL3 plus brusatol against NSCLC was also evaluated *in vivo*. Similar to the *in vitro* results, we noticed the combination of brusatol and erastin, or brusatol and RSL3, showed better therapeutic function than single erastin or RSL3 treatment. The combination treatment increased the survival rate and decreased the growth of tumor obviously (Fig. 7A–B). Even though the combination of brusatol and RSL3 didn't show different

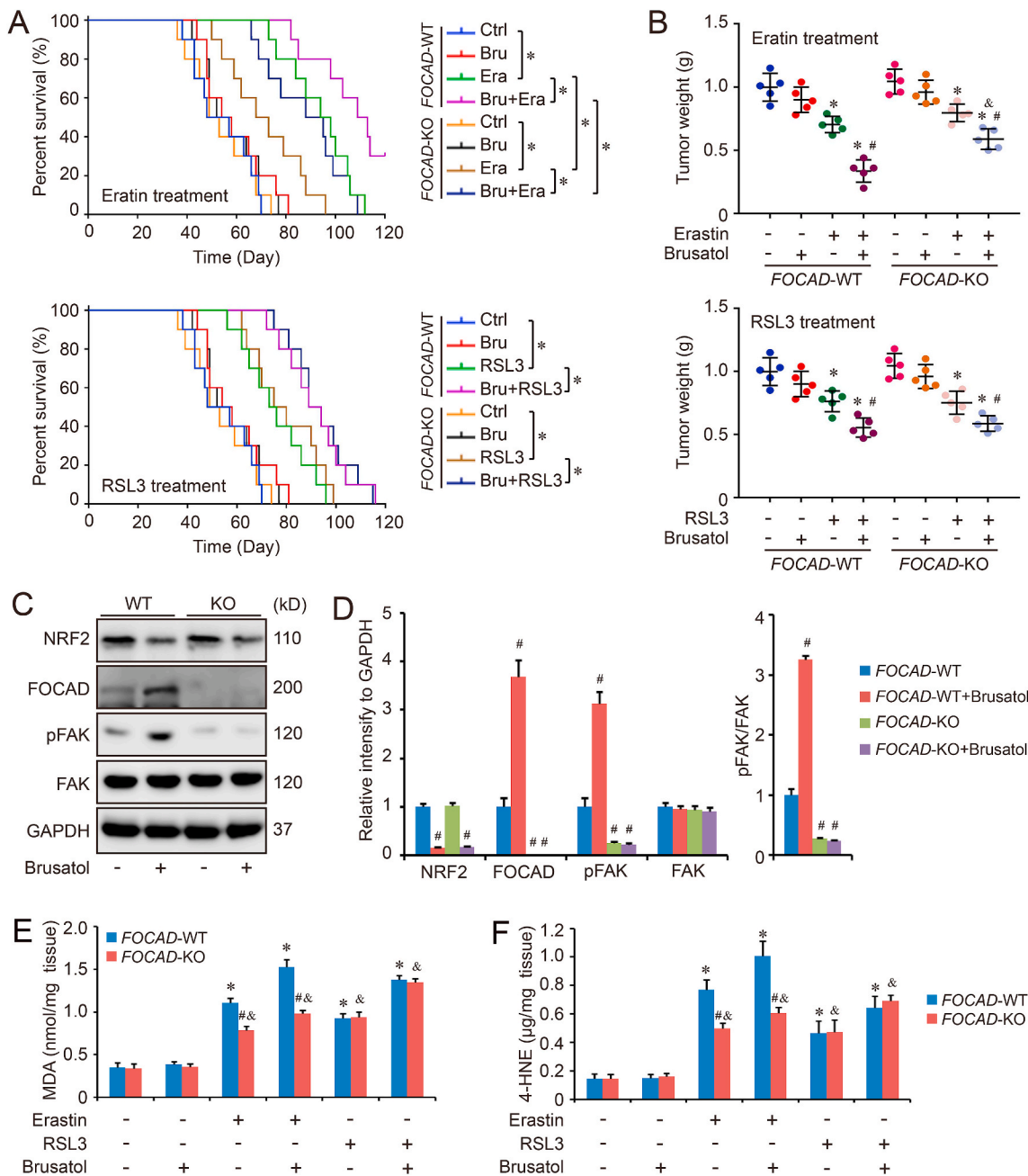


Fig. 7. Anti-tumor efficacy of ferroptosis inducers and brusatol in xenograft mouse model. *FOCAD*-Wild type (*FOCAD*-WT) and *FOCAD*-knockout (*FOCAD*-KO) A549 cells were injected into NOG mice, and the mice were further treated with erastin (Era), RSL3, and brusatol (Bru). The survival rate (n = 10) within 120 days was also evaluated in different groups (A). The univariate cox proportional hazard regression assay was performed to compare the difference of survival rate between different groups. *: P < 0.05 compared between two different groups. In addition, the mice were sacrificed and tumor weight (n = 5) was measured in each group (B). The effect of Brusatol treatment on *FOCAD*-FAK signaling in the tumor tissues was measured with western blot (C–D), and the levels of MDA (E) and 4-HNE (F) in the tumor tissues were measured respectively to evaluate ferroptosis in different groups. Results were expressed as mean ± SD, and the P value less than 0.05 was considered statistically significant. In Fig. 7A, *: P < 0.05 compared between two groups. In Fig. 7B, *: P < 0.05 compared with Erastin(-)Brusatol(-) group or RSL3 (-)Brusatol(-) group in same genotype. #: P < 0.05 compared with Erastin(+)-Brusatol(-) group or RSL3(+)-Brusatol(-) group in same genotype. &: P < 0.05 compared between *FOCAD*-WT group and *FOCAD*-KO group in same condition. In Fig. 7D, #: P < 0.05 compared with *FOCAD*-WT group. In Fig. 7E–F, *: P < 0.05 compared with the *FOCAD*-WT group in the first condition. #: P < 0.05 compared between *FOCAD*-WT group and *FOCAD*-KO group in same condition. &: P < 0.05 compared with the *FOCAD*-KO group in the first condition.

therapeutic action against *FOCAD*-WT and *FOCAD*-KO NSCLC cells, the therapy function of brusatol + erastin was limited against *FOCAD*-KO NSCLC cells compared with *FOCAD*-WT NSCLC cells (Fig. 7A–B). Moreover, *FOCAD*-FAK signaling was further evaluated in the tumor tissues. We also found that brusatol treatment increased the level of *FOCAD* and promoted pAKT signaling via affecting NRF2, which was abolished by *FOCAD* knockout (Fig. 7C–7D). Besides, the combination of brusatol and RSL3 didn't show different effect on ferroptosis in *FOCAD*-WT group and *FOCAD*-KO group, but the ferroptosis induced by signal erastin or brusatol + erastin was limited in *FOCAD*-KO group compared with *FOCAD*-WT group, indicating the key position of *FOCAD* in cysteine deprivation-induced ferroptosis (Fig. 7E–F).

4. Discussion

As a novel regulated cell death, ferroptosis gradually attracts lots of scientists' attention in recent years. However, the detailed mechanistic insights into the ferroptosis regulation remain unclear in different disease contexts. Recently, several studies indicated that many components of the ferroptosis cascade, such as *GPX4*, *SLC7A11* and *GST*, were the downstream genes of NRF2 [17–20]. Therefore, NRF2 should hold a critical role in the regulation of ferroptotic response. In this study, we mainly explored the position of NRF2-*FOCAD*-FAK signaling in cellular response to ferroptosis. Our results indicated that NRF2 negatively regulated the transcription of *FOCAD* gene that was essential for the activity of FAK. The inhibition of FAK activity blocked the mitochondrial TCA cycle and the Complex I activity in mitochondrial ETC, and further reduced the cellular sensitivity to cysteine deprivation-induced ferroptosis, but not *GPX4* inhibition-induced ferroptosis in NSCLC cells. Therefore, NRF2 inhibitor (brusatol) improved the therapeutic action of erastin against NSCLC via suppressing the expression of anti-ferroptosis genes and activating the *FOCAD*-FAK signaling pathway (Fig. 8).

Ferroptosis was initially characterized by the pathological changes of mitochondria, such as the decreased mitochondrial volume as well as the condensed density of mitochondrial membrane [1,39,40]. Thus, the correlation between mitochondria and ferroptosis has been investigated by scientists in recent years. For example, both mitochondrial ROS production and mitochondrial damage are related with ferroptosis [1], and mitochondria is also regarded as one of the most important target for ferroptosis activators or inhibitors [41]. However, some groups also show opposite results against the central role of mitochondria in ferroptosis. Gaschler MM et al. investigated the functional relationship between mitochondria and ferroptosis inhibition induced by ferrostatins. They noticed that mitochondria were unnecessary for such ferroptosis regulation, while endoplasmic reticulum might hold a more important potential in the suppression of ferroptosis [42]. Therefore, the accurate function of mitochondria in ferroptosis regulation could be varied in different models. Recently, Gao et al. investigated the position of mitochondria in ferroptosis intensively. They found that mitochondria indeed hold an important potential in cysteine deprivation-induced ferroptosis, but not in *GPX4* inhibition-induced ferroptosis. Moreover, both mitochondrial ETC activity and TCA cycle were essential for lipid ROS production in cysteine deprivation-induced ferroptosis. Therefore, the suppression of those canonical metabolic activity in mitochondria effectively relieved the ferroptosis induced by erastin or cystine starvation, indicating the close functional relevance between mitochondria and ferroptosis [32]. Our study also confirmed the conclusion about mitochondria and cysteine deprivation-induced ferroptosis. We found *FOCAD* promoted mitochondrial function via increasing FAK activity, which enhanced the sensitivity to erastin-induced ferroptosis in NSCLC cells. However, *FOCAD* didn't affect the cellular response to RSL3-induced ferroptosis *in vitro* and *in vivo*. In addition, the position of *FOCAD* in ferroptosis was also evaluated in BEAS-2B cells (bronchial epithelial cell line), because of the different metabolic phenotype between cancer cells and primary cells. Even though the results are similar to that in NSCLC cells, whether the detailed mechanisms are consistent

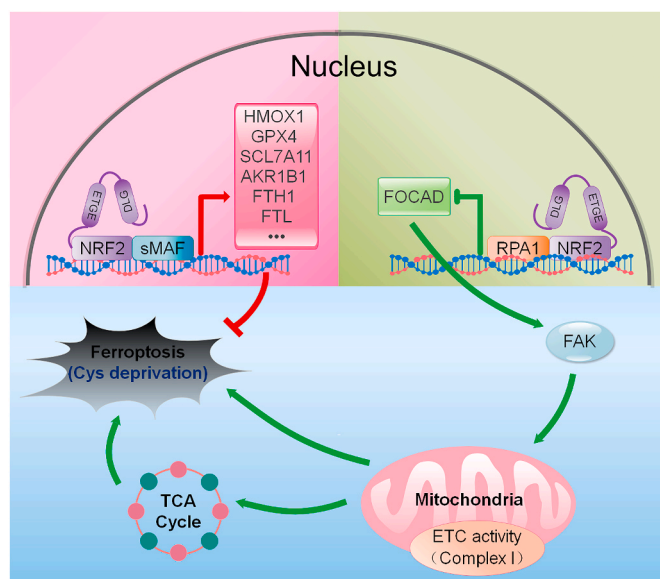


Fig. 8. Proposed model for the relationship between NRF2-*FOCAD*-FAK signaling and cysteine deprivation-induced ferroptosis. Lots of components of the ferroptosis cascade, such as *GPX4*, *SLC7A11*, and *AKR1B1*, could be positively regulated by NRF2. In addition, NRF2 negatively regulated the transcription of *FOCAD* gene that was essential for the activity of FAK, and the suppression of FAK activity reduced the cellular sensitivity to cysteine (Cys) deprivation-induced ferroptosis via affecting the mitochondrial TCA cycle and the activity of Complex I in mitochondrial ETC.

still needs our further investigation.

NRF2 is a master transcription factor for the expression of multiple antioxidant genes. Besides, NRF2 also contributes to the regulation of mitochondrial function via some divergent intermolecular linkages. For example, NRF2 directly upregulates the expression of mitochondrial transcription factors, and promotes mitochondrial biogenesis. Meanwhile, some mitochondrial proteins also join in the regulation of NRF2 and form a reciprocal regulatory loop between NRF2 and mitochondria [43,44]. Brusatol is the first inhibitor in NRF2 signaling pathway. Recently, some researcher found that both intracellular ROS level and mitochondrial ROS level could be reduced by the treatment with brusatol, and brusatol also improved mitochondrial function and suppressed the release of cytochrome c, ameliorating the mitochondrial respiratory dysfunction caused by the overload of ROS [45,46]. However, why the downregulation of NRF2 could result in the mitochondrial protective effect remains unclear. In our study, we also noticed the effect of brusatol on mitochondrial TCA cycle and mitochondrial ETC, which was based on the regulation of *FOCAD* and FAK activity, providing a novel insight into the relationship between mitochondria and NRF2. In addition, the combination of ferroptosis inducer and brusatol may be a promising therapy mode against cancer in clinic as well. We found that the combination of erastin and brusatol, or combination of RSL and brusatol, showed better therapeutic action against lung cancer than single erastin or RSL treatment. However, the dose of brusatol we used in our study was so low (50 nM *in vitro*, and 0.5 mg/kg *in vivo*) that it's not enough to cause obvious cellular toxicity or ferroptosis, even though it inhibited NRF2 signaling and enhanced the anti-cancer function of erastin or RSL effectively (Figs. 6–7). Therefore, the effect of co-treatment with brusatol and erastin/RSL on cancer cell growth or ferroptosis, is stronger than single erastin/RSL effect plus single brusatol effect. It could be possible that there is a synergistic relationship between brusatol and erastin/RSL. However, only one dose for each compound was applied in our study, and the synergistic relationship as well as the related mechanism still need to be investigated using different doses in multiple models *in vivo* and *in vitro*.

FAK, a cytoplasmic protein tyrosine kinase, holds an essential position during the process of embryonic development [47,48]. Besides, lots of studies have suggested the importance of FAK in the pathogenesis of different human diseases [49,50]. In recent years, the relationship between FAK and mitochondria was also investigated by some scientists. Visavadiya NP et al. found that either pharmacological inhibition or siRNA inhibition of FAK could abolish mitochondrial function effectively, which was dependent of the regulation of STAT3 [37]. Moreover, the inhibition of FAK-STAT3 signaling pathway also promoted the mitochondrial dysfunction and cell death caused by endoplasmic reticulum stress in endothelial cells [34]. Besides, FAK silencing suppressed mitochondrial biogenesis via the downregulation of PGC-1 α , NRF-1, and mtDNA [36]. Therefore, FAK is essential for the mitochondrial function. In this study, our results also confirmed the function of FAK in mitochondrial regulation. We found the increased activity of FAK promoted mitochondrial TCA cycle and mitochondrial ETC, which enhanced the sensitivity to erastin-induced ferroptosis in NSCLC cells. However, the detailed mechanism still needs our further exploration. In addition, we found FAK signaling was positively regulated by FOCAD. However, the treatment of PF-573228 (a FAK signaling inhibitor) didn't affect the level of FOCAD in either FOCAD-WT group or FOCAD-OE group (Fig. 5C), which indicated that FOCAD is the upstream of FAK signaling, and FAK signaling may not regulate FOCAD.

Our study mainly indicated the significance of NRF2-FOCAD-FAK signaling pathway in the regulation of ferroptosis. To further analyze the clinical significance of each gene, the mRNA transcripts were compared between tumor tissues and normal tissues using TCGA database. Herein, lung squamous cell carcinoma (LUSC) and lung adenocarcinoma (LUAD), two most major subtypes of NSCLC, were chosen to perform the assay. However, no significant difference could be found between tumor tissues and normal lung tissues (Fig. S8A). In addition, the relevance between those genes and patients' overall survival rate/disease free survival rate was evaluated respectively. The low expression and high expression of each gene were determined by the median value of mRNA transcripts per million (TPM). The univariate cox proportional hazard regression assay suggested that the mRNA levels of NRF2, FOCAD or FAK were not related with the survival rate in either LUAD patients or LUSC patients (Figs. S8B–S8D), even though the protein levels of NRF2 and FOCAD showed negative relationship in cancer tissues and paracancer tissues (Fig. 1A–C). It could be possible that some unclear mechanisms in posttranslational modification hold more important potential in the regulation of NRF2-FOCAD-FAK. Moreover, the ferroptosis inducers, such as erastin and RSL3, haven't been widely used in the clinical treatment against NSCLC so far, and the patients in TCGA database also received different treatment. Therefore, it will be more convincing if the survival comparison was performed based on NSCLC patients treated with similar ferroptosis inducers.

5. Conclusion

In conclusion, this study mainly addressed the link between NRF2-FOCAD-FAK signaling pathway and ferroptosis in human NSCLC model. NRF2 negatively regulated FOCAD-FAK signaling that strengthens the sensitivity of NSCLC cells to cysteine deprivation-induced ferroptosis, via improving mitochondrial TCA cycle as well as Complex I activity in mitochondrial ETC, while FOCAD-FAK signaling didn't show obvious effect on GPX4 inhibition-induced ferroptosis. In addition, the treatment with NRF2 inhibitor, brusatol, increased the therapeutic action of ferroptosis inducer against NSCLC, which partially depended on the activation of FOCAD-FAK signaling pathway. Even though the crosstalk among NRF2-FOCAD-FAK, mitochondria, and ferroptosis needs our further investigation, our current research provides a novel insight into ferroptosis-based treatment for human NSCLC.

Declaration of competing interest

The authors declare that there are no conflicts of interest.

Acknowledgement

This study was supported by National Natural Science Foundation of China (31900547), Project funded by China Postdoctoral Science Foundation (2019M653277, 2020T130250) and The grants from Shenzhen Peacock Plan (KQTD2016113015442590).

Appendix A. Supplementary data

Supplementary data to this article can be found online at <https://doi.org/10.1016/j.redox.2020.101702>.

References

- [1] S.J. Dixon, K.M. Lemberg, M.R. Lamprecht, R. Skouta, E.M. Zaitsev, C.E. Gleason, et al., Ferroptosis: an iron-dependent form of nonapoptotic cell death, *Cell* 149 (2012) 1060–1072.
- [2] B.R. Stockwell, J.P. Friedmann Angeli, H. Bayir, A.I. Bush, M. Conrad, S.J. Dixon, et al., Ferroptosis: a regulated cell death nexus linking metabolism, redox biology, and disease, *Cell* 171 (2017) 273–285.
- [3] K. Bersuker, J.M. Hendricks, Z. Li, L. Magtanong, B. Ford, P.H. Tang, et al., The CoQ oxidoreductase FSP1 acts parallel to GPX4 to inhibit ferroptosis, *Nature* 575 (2019) 688–692.
- [4] S. Doll, F.P. Freitas, R. Shah, M. Aldrovandi, M.C. da Silva, I. Ingold, et al., FSP1 is a glutathione-independent ferroptosis suppressor, *Nature* 575 (2019) 693–698.
- [5] P. Lei, T. Bai, Y. Sun, Mechanisms of ferroptosis and relations with regulated cell death: a review, *Front. Physiol.* 10 (2019) 139.
- [6] T. Xu, W. Ding, X. Ji, X. Ao, Y. Liu, W. Yu, et al., Molecular mechanisms of ferroptosis and its role in cancer therapy, *J. Cell Mol. Med.* 23 (2019) 4900–4912.
- [7] Z.Z. Shi, Z.W. Fan, Y.X. Chen, X.F. Xie, W. Jiang, W.J. Wang, et al., Ferroptosis in carcinoma: regulatory mechanisms and New method for cancer therapy, *OncoTargets Ther.* 12 (2019) 11291–11304.
- [8] S. Masaldan, A.A. Belaidi, S. Ayton, A.I. Bush, Cellular senescence and iron dyshomeostasis in alzheimer's disease, *Pharmaceuticals* 12 (2019) 93.
- [9] Q. Li, X. Han, X. Lan, Y. Gao, J. Wan, F. Durham, et al., Inhibition of neuronal ferroptosis protects hemorrhagic brain, *JCI Insight* 2 (2017), e90777.
- [10] X. Guan, X. Li, X. Yang, J. Yan, P. Shi, L. Ba, et al., The neuroprotective effects of carvacrol on ischemia/reperfusion-induced hippocampal neuronal impairment by ferroptosis mitigation, *Life Sci.* 235 (2019) 116795.
- [11] P. Liu, Y. Feng, H. Li, X. Chen, G. Wang, S. Xu, et al., Ferrostatin-1 alleviates lipopolysaccharide-induced acute lung injury via inhibiting ferroptosis, *Cell. Mol. Biol. Lett.* 25 (2020) 10.
- [12] J.P. Friedmann Angeli, D.V. Krysko, M. Conrad, Ferroptosis at the crossroads of cancer-acquired drug resistance and immune evasion, *Nat. Rev. Canc.* 19 (2019) 405–414.
- [13] A. Lau, N.F. Villeneuve, Z. Sun, P.K. Wong, D.D. Zhang, Dual roles of Nrf2 in cancer, *Pharmacol. Res.* 58 (2008) 262–270.
- [14] N.F. Villeneuve, A. Lau, D.D. Zhang, Regulation of the Nrf2-Keap1 antioxidant response by the ubiquitin proteasome system: an insight into cullin-ring ubiquitin ligases, *Antioxidants Redox Signal.* 13 (2010) 1699–1712.
- [15] S. Menegon, A. Columbano, S. Giordano, The dual roles of NRF2 in cancer, *Trends Mol. Med.* 22 (2016) 578–593.
- [16] E.J. Moon, A. Giaccia, Dual roles of NRF2 in tumor prevention and progression: possible implications in cancer treatment, *Free Radic. Biol. Med.* 79 (2015) 292–299.
- [17] W.O. Osburn, N. Wakabayashi, V. Misra, T. Nilles, S. Biswal, M.A. Trush, et al., Nrf2 regulates an adaptive response protecting against oxidative damage following diquat-mediated formation of superoxide anion, *Arch. Biochem. Biophys.* 454 (2006) 7–15.
- [18] T. Ishii, K. Itoh, S. Takahashi, H. Sato, T. Yanagawa, Y. Katoh, et al., Transcription factor Nrf2 coordinately regulates a group of oxidative stress-inducible genes in macrophages, *J. Biol. Chem.* 275 (2000) 16023–16029.
- [19] M.J. Kerins, A. Ooi, The roles of NRF2 in modulating cellular iron homeostasis, *Antioxidants Redox Signal.* 29 (2018) 1756–1773.
- [20] M. Dodson, R. Castro-Portuguez, D.D. Zhang, NRF2 plays a critical role in mitigating lipid peroxidation and ferroptosis, *Redox Biol* 23 (2019) 101107.
- [21] C. Tonelli, I.L.C. Chio, D.A. Tuveson, Transcriptional regulation by Nrf2, *Antioxidants Redox Signal.* 29 (2018) 1727–1745.
- [22] P. Liu, M. Rojo de la Vega, S. Sammani, J.B. Mascarenhas, M. Kerins, M. Dodson, et al., RPA1 binding to NRF2 switches ARE-dependent transcriptional activation to ARE-NRE-dependent repression, *Proc. Natl. Acad. Sci. U. S. A.* 115 (2018) E10352–E10361.
- [23] A. Brockschmidt, D. Trost, H. Peterziel, K. Zimmermann, M. Ehrler, H. Grassmann, et al., KIAA1797/FOCAD encodes a novel focal adhesion protein with tumour suppressor function in gliomas, *Brain* 135 (2012) 1027–1041.

- [24] F. Brand, A. Forster, A. Christians, M. Bucher, C.M. Thome, M.S. Raab, et al., FOCAD loss impacts microtubule assembly, G2/M progression and patient survival in astrocytic gliomas, *Acta Neuropathol.* 139 (2020) 175–192.
- [25] P. Liu, Y. Feng, X. Chen, G. Wang, I. Nawaz, L. Hu, et al., Paracrine action of human placental trophoblast cells attenuates cisplatin-induced acute kidney injury, *Life Sci.* 230 (2019) 45–54.
- [26] L. Zhao, X. Chen, Y. Feng, G. Wang, I. Nawaz, L. Hu, et al., COX7A1 suppresses the viability of human non-small cell lung cancer cells via regulating autophagy, *Canc. Med.* 8 (2019) 7762–7773.
- [27] P. Liu, W. Tian, S. Tao, J. Tillotson, E.M.K. Wijeratne, A.A.L. Gunatilaka, et al., Non-covalent NRF2 activation confers greater cellular protection than covalent activation, *Cell Chem. Biol.* 26 (2019) 1427–1435.
- [28] S. Tao, P. Liu, G. Luo, M. Rojo de la Vega, H. Chen, T. Wu, et al., p97 negatively regulates NRF2 by extracting ubiquitylated NRF2 from the KEAP1-CUL3 E3 complex, *Mol. Cell Biol.* 37 (2017) e00660-16.
- [29] L. Zhao, Y. Feng, X. Chen, J. Yuan, X. Liu, Y. Chen, et al., Effects of IGF-1 on neural differentiation of human umbilical cord derived mesenchymal stem cells, *Life Sci.* 151 (2016) 93–101.
- [30] T. Wu, X.J. Wang, W. Tian, M.C. Jaramillo, A. Lau, D.D. Zhang, Poly(ADP-ribose) polymerase-1 modulates Nrf2-dependent transcription, *Free Radic. Biol. Med.* 67 (2014) 69–80.
- [31] A.M. Erickson, Z. Neveara, J.J. Gipp, R.T. Mulcahy, Identification of a variant antioxidant response element in the promoter of the human glutamate-cysteine ligase modifier subunit gene. Revision of the ARE consensus sequence, *J. Biol. Chem.* 277 (2002) 30730–30737.
- [32] M. Gao, J. Yi, J. Zhu, A.M. Minikes, P. Monian, C.B. Thompson, et al., Role of mitochondria in ferroptosis, *Mol. Cell.* 73 (2019) 354–363.
- [33] V. Desquiret-Dumas, N. Gueguen, G. Leman, S. Baron, V. Nivet-Antoine, S. Chupin, et al., Resveratrol induces a mitochondrial complex I-dependent increase in NADH oxidation responsible for sirtuin activation in liver cells, *J. Biol. Chem.* 288 (2013) 36662–36675.
- [34] K. Banerjee, M.P. Keasey, V. Razskazovskiy, N.P. Visavadiya, C. Jia, T. Hagg, Reduced FAK-STAT3 signaling contributes to ER stress-induced mitochondrial dysfunction and death in endothelial cells, *Cell. Signal.* 36 (2017) 154–162.
- [35] C.C. Tseng, Y.C. Lai, T.J. Kuo, J.H. Su, P.J. Sung, C.W. Feng, et al., Rhodoptilometrin, a crinoid-derived anthraquinone, induces cell regeneration by promoting wound healing and oxidative phosphorylation in human gingival fibroblast cells, *Mar. Drugs* 17 (2019) 138.
- [36] T.F. Tornatore, A.P. Dalla Costa, C.F. Clemente, C. Judice, S.A. Rocco, V. C. Calegari, et al., A role for focal adhesion kinase in cardiac mitochondrial biogenesis induced by mechanical stress, *Am. J. Physiol. Heart Circ. Physiol.* 300 (2011) H902–H912.
- [37] N.P. Visavadiya, M.P. Keasey, V. Razskazovskiy, K. Banerjee, C. Jia, C. Lovins, et al., Integrin-FAK signaling rapidly and potently promotes mitochondrial function through STAT3, *Cell Commun. Signal.* 14 (2016) 32.
- [38] D. Ren, N.F. Villeneuve, T. Jiang, T. Wu, A. Lau, H.A. Toppin, et al., Brusatol enhances the efficacy of chemotherapy by inhibiting the Nrf2-mediated defense mechanism, *Proc. Natl. Acad. Sci. U. S. A.* 108 (2011) 1433–1438.
- [39] J. Du, Y. Zhou, Y. Li, J. Xia, Y. Chen, S. Chen, et al., Identification of Frataxin as a regulator of ferroptosis, *Redox Biol.* 32 (2020) 101483.
- [40] J. Liu, F. Kuang, G. Kroemer, D.J. Klionsky, R. Kang, D. Tang, Autophagy-dependent ferroptosis: machinery and regulation, *Cell Chem. Biol.* 27 (2020) 420–435.
- [41] T. Krainz, M.M. Gaschler, C. Lim, J.R. Sacher, B.R. Stockwell, P. Wipf, A mitochondrial-targeted nitroxide is a potent inhibitor of ferroptosis, *ACS Cent. Sci.* 2 (2016) 653–659.
- [42] M.M. Gaschler, F. Hu, H. Feng, A. Linkermann, W. Min, B.R. Stockwell, Determination of the subcellular localization and mechanism of action of ferrostatins in suppressing ferroptosis, *ACS Chem. Biol.* 13 (2018) 1013–1020.
- [43] S. Kovac, P.R. Angelova, K.M. Holmstrom, Y. Zhang, A.T. Dinkova-Kostova, A. Y. Abramov, Nrf2 regulates ROS production by mitochondria and NADPH oxidase, *Biochim. Biophys. Acta* 1850 (2015) 794–801.
- [44] I.G. Ryou, M.K. Kwak, Regulatory crosstalk between the oxidative stress-related transcription factor Nfe2l2/Nrf2 and mitochondria, *Toxicol. Appl. Pharmacol.* 359 (2018) 24–33.
- [45] S. Zhu, S. Liu, L. Wang, W. Ding, J. Sha, H. Qian, et al., Brusatol protects HepG2 cells against oxygen-glucose deprivation-induced injury via inhibiting mitochondrial reactive oxygen species-induced oxidative stress, *Pharmacology* (2019) 1–8.
- [46] Y. Lu, B. Wang, Q. Shi, X. Wang, D. Wang, L. Zhu, Brusatol inhibits HIF-1 signaling pathway and suppresses glucose uptake under hypoxic conditions in HCT116 cells, *Sci. Rep.* 6 (2016) 39123.
- [47] M. Luo, J.L. Guan, Focal adhesion kinase: a prominent determinant in breast cancer initiation, progression and metastasis, *Canc. Lett.* 289 (2010) 127–139.
- [48] R.C. Ransom, A.C. Carter, A. Salhotra, T. Leavitt, O. Marecic, M.P. Murphy, et al., Mechanoresponsive stem cells acquire neural crest fate in jaw regeneration, *Nature* 563 (2018) 514–521.
- [49] H. Jiang, S. Hegde, B.L. Knolhoff, Y. Zhu, J.M. Herndon, M.A. Meyer, et al., Targeting focal adhesion kinase renders pancreatic cancers responsive to checkpoint immunotherapy, *Nat. Med.* 22 (2016) 851–860.
- [50] B.Z. Carter, P.Y. Mak, X. Wang, H. Yang, G. Garcia-Manero, D.H. Mak, et al., Focal adhesion kinase as a potential target in AML and MDS, *Mol. Canc. Therapeut.* 16 (2017) 1133–1144.